Melting and Crystallization Behavior of Poly(ethylene terephthalate) and Poly(*m*-xylylene adipamide) Blends

Fei Xie, Elizabeth A. Lofgren, Saleh A. Jabarin

Polymer Institute and Department of Chemical and Environmental Engineering, College of Engineering, The University of Toledo, Toledo, Ohio 43606-3390

Received 17 July 2009; accepted 26 March 2010
DOI 10.1002/app.32526
Published online 11 June 2010 in Wiley InterScience (www.interscience.wiley.com).

ABSTRACT: The crystallization and melting behaviors as well as the crystalline morphologies of Poly(ethylene terephthalate)/Poly(*m*-xylylene adipamide) (PET/MXD6) blends have been examined and characterized with the aid of differential scanning calorimetry (DSC) and wide angle x-ray diffraction (WAXD). The isothermal and nonisothermal crystallization behaviors of the blends were studied as functions of the contents of MXD6, catalyst concentrations, and the effects of the interchange reactions between PET and MXD6. Wide angle x-ray scattering has been used to examine the crystalline morphologies of the PET/MXD6 blends, to characterize their crystalline and amorphous phases, and to determine crystallite sizes in the blends. Results indicate that the catalyst has both catalyzing and nucleation effects on the PET/MXD6 blends, with the extents of each effect dependent upon the content of catalyst. In addition the crystalline morphology was found to be dominated by the MXD6 content as well as the crystallization temperature. © 2010 Wiley Periodicals, Inc. J Appl Polym Sci 118: 2153–2164, 2010

Key words: poly(ethylene terephthalate); poly(*m*-xylylene adipamide); diluent effect; crystallization; crystallite size

INTRODUCTION

As a semicrystalline polymer, poly(ethylene terephthalate) (PET), exhibits various properties that are dependent upon its melting and crystallization behaviors. The melting characteristics of a PET material are primarily related to its relative level of crystallinity and previous heat history. PET samples with the same degree of crystallinity may exhibit different melting characteristics. These differences are often indicated by the existence of multiple melting endotherms, recorded during differential scanning calorimetry (DSC) measurements. The multiple melting endothermic phenomenon, observed by many researchers,[1–10] is not restricted to PET, but has also been found for other polycondensation polymers such as nylon 66,[11] PEEK,[12–17] and PEN.[18]

Polymer blends consisting of two crystallizable components may be classified in terms of amorphous/amorphous, crystalline/amorphous, and crystalline/crystalline systems. There are three important factors[19–21] that can influence the morphologies of blends. The first of these factors comprises polymer–polymer specific interactions, which include interactions among the functional groups of the two polymer blend components. The second factor is related to the cooperative diffusion coefficient, which is the ratio of the polymer diffusivities in the blends. The third factor is controlled by the separation distance of the segregation of amorphous diluent, which is related to the magnitude of the amorphous phase. As a result of these three factors, crystalline/amorphous systems may display various combinations of interlamellar, interfibrillar, and/or interspherulitic morphologies.[21] In the case of interlamellar blend morphologies, the amorphous component resides between the crystalline lamellae. For interfibrillar morphologies, the amorphous component can be incorporated within the spherulites and in the case of interspherulitic morphologies, the amorphous component would be rejected from the spherulites. These different polymer blend morphologies can generally coexist.

In the case of two component polymer blends; in which only one of them is crystalline, the parameters controlling the specific locations of the amorphous phases are not yet fully understood. Some researchers[19–36] have proposed that there are two forces controlling the positions of molecules in the amorphous phase. One of these is the confinement of the amorphous molecules by the spherulite lamellae. This leads to an entropic driving force, which tends to pull molecules in the amorphous phase out of the interlamellar regions and is associated with

Correspondence to: S. A. Jabarin (saleh.jabarin@utoledo.edu).

Contract grant sponsor: PET Industrial Research Consortium.

their tendency to resume random-coiled conformations. Another controlling force is the crystallization driving force of the crystallizable segments within the interlamellar zones. This force pushes the amorphous molecules out of the interlamellar regions and into the interspherulitic regions. Both of these forces reject molecules of the amorphous component from within the interlamellar zones.

In addition, there are three factors which govern the exclusion of amorphous component molecules from within the interlamellar regions. These include the magnitude of the interaction parameter (χ), the interlamellar distance (which determines the extent to which the amorphous molecules are deformed), and the degree of supercooling (which determines the driving force of crystallization). All these factors depends on polymer blend composition, exposure temperature, and molecular weight.

Chain diffusivity[19,20] is another important kinetic factor in blend morphology. It has been suggested that the distance over which an uncrystallizable impurity may be segregated, is determined by the relative magnitude of the diffusion coefficient (D) of the impurity molecules as well as by the crystal growth rate (G) of the crystallizable phase. If the diffusion rate of the amorphous component molecules is relatively slower than the crystal growth rate, then these molecules may be trapped inside the interlamellar regions of the crystallizable component, before they have a chance to diffuse out. The relationship between D and G is defined by the parameter (δ), where $\delta = D/G$. The δ term has the unit of length and thus provides a qualitative measure of segregation distance. As with exclusion of the amorphous component, δ is also dependent on composition, temperature, and molecular weight.

Morphologies described in terms of crystalline/amorphous component behaviors have been observed in blends of poly(aryl ether ketones) (PAEK)/poly(ether imide) (PEI),[21] poly(ethylene oxide) (PEO)/poly(methyl methacrylate)(PMMA),[19,20] poly(ε-caprolactone)/polycarbonate[22–25] polyamide 6/polyarylate,[26] poly(butylene terephthalate)/polyarylate,[27–29] PET/polycarbonate,[30] PET/polyarylate,[31] PET/poly(ethylene 2,6-naphthalate) (PEN),[32,33] polycaprolactone (PCL)/poly(vinyl chloride) (PVC),[34] and poly(vinylidene fluoride) (PVF_2)/PMMA.[35,36]

In the case of crystalline/crystalline blends, cocrystallization is unfavorable because it requires close matching of chain conformations and lattice parameters. Crystallization of the two components generally creates two species of crystals, whose morphologies are characterized by their arrangement with respect to each other. These species may exist in either an insertion mode or a block mode. In the case of insertion mode arrangements, the different crystals randomly mix together in the lamellar stacks (LS). In block mode arrangements, the two different crystal species form respective LS domains. During crystallization, the common exclusion distance of the two components governs the formation of these morphological patterns.[37,38] The insertion mode is induced by the mutual segregation distance comparable to the lamellar thickness, which is on the order of several nanometers. The block mode is characterized by longer segregation distances, on the order of tens of nanometers to microns.

The most widely studied crystalline/crystalline systems include blends of high-density polyethylene (HDPE) and low-density polyethylene (LDPE).[39] In these blends, the intermolecular interactions between the two components are very small. In comparison with other polymer blends, the blends of HDPE and LDPE are ideal. Other crystalline/crystalline blends include materials such as: polypropylene/polyethylene,[37] poly(butylene terephthalate) (PBT)/polyarylate,[38,40] PBT/poly(ethylene oxide),[41] nylon 6/liquid crystal copolyester,[42] poly(vinylidene fluoride)/polyamide 6,[43] poly(vinylidene fluoride)/poly(4-hydroxybutyrate) (PHB),[44] poly(4-hydroxybutyrate) (PHB)/poly(ethylene oxide) (PEO),[45] poly(ethylene oxide) (PEO)/poly(ethylene succinate) (PES),[46] PET/PBT,[47] poly(vinylidene fluoride)/poly(1,4-butylene adipate),[48–50] and PET/liquid crystal polyester (Vectra A).[51]

PET and poly(*m*-xylylene adipamide) (MXD6) are both semicrystalline polymers. When they are blended together, the previously discussed morphological changes should be considered. As described in the previous study on the interchange reaction of PET/MXD6 blends,[52] we have shown that PET can react with MXD6 in the presence of sodium *p*-toluenesulfonate catalyst. The influence of the interchange reactions on the thermal properties and morphologies of these blends is the subject of current investigations. To elucidate these characteristics of the PET/MXD6 blends, crystallization behaviors and equilibrium melting temperatures have been examined with the aid of DSC. The morphologies of selected crystallized samples have also been characterized using wide angle x-ray diffraction (WAXD).

EXPERIMENTAL

Materials used for this work include Voridian Aqua WA314 PET, with a number average molecular weight of 25,800 g/mol and intrinsic viscosity of 0.75 dL/g. The poly(*m*-xylylenadipamide) 6007 MXD6, from Mitsubishi Gas Chemical, had a number average molecular weight of 25,900 g/mol and a relative viscosity of 2.7 dL/g. These resins were chosen for blending to achieve a close melt viscosity

TABLE I
Compositions of the Prepared PET/MXD6 Blends

	Catalyst content (wt %)				
PET/MXD6	0	0.5	1	3	5
100/0	√				√
99/1	√	√			
97/3	√	√			
95/5	√	√			
90/10	√	√	√	√	√
85/15	√	√			
80/20	√	√			
70/30	√				
60/40	√				
50/50	√				
40/60	√				
0/100	√				

match. The sodium *p*-toluenesulfonate catalyst was purchased from Sigma Aldrich. All materials were dried in a vacuum oven at 120°C for at least 20 h to moisture levels of less than 0.005%, before being processed. As previously described,[52] a Hakke Rheomex single screw extruder was used to prepare a master batch of sodium *p*-toluenesulfonate catalyst in PET, at a concentration of 5% (wt/wt). This master batch was used in conjunction with the PET and MXD6 materials to prepare the desired blend compositions. A Werner and Pfleiderer (ZSF-30) self-wiping co-rotating twin-screw extruder was used for all other melt blending operations. Blends were prepared with various concentrations of PET and MXD6 and with catalyst contents from 0 to 5% (wt/wt) as shown in Table I.

A Perkin–Elmer differential scanning calorimeter (DSC 7) was used to measure the nonisothermal and isothermal crystallization behavior of PET/MXD6 blends that had previously been vacuum-dried overnight at 120°C. Samples characterized in terms of nonisothermal crystallization were first heated from 40 to 300°C at 320°C/min and then held for 5 min at 300°C to remove previous crystallinity and heat history. They were then cooled from 300°C to 40°C at rates from 5 to 100°C/min to record their dynamic crystallization behaviors.

Isothermal crystallization was monitored using samples that had first been heated from 40 to 300°C at 320°C/min and held for 5 min at 300°C. These melted samples were quickly cooled from 300°C to the specified isothermal crystallization temperatures from 180 to 225°C and their crystallization behaviors were recorded as functions of time. The samples were held at each temperature for sufficient time to allow complete crystallization to occur and then cooled to 40 at 320°C/min. The cooled samples were then heated from 40 to 300°C at 10°C/min to record the melting behaviors of the previously formed crystallinity. Differences in these resulting endotherms were utilized for calculation of equilibrium melting temperatures.

A wide angle x-ray powder diffractometer was used to further investigate the morphologies of the polymer blends. The amorphous samples with different contents of MXD6 and containing 0–5% catalyst were ground into a fine powder with a small electric grinder cooled with liquid nitrogen, to prepare them for x-ray analysis. These samples were then dried in a vacuum oven at 30°C for at least 48 h. The amorphous dried, ground, samples were then crystallized under vacuum at selected isothermal temperatures from 180 to 210°C. Temperatures were monitored with a thermocouple placed near the sample containers. After the recorded sample temperatures were equal to the selected isothermal crystallization temperatures, timing was initiated to obtain isothermal crystallization times from 10 to 120 min. X-ray diffraction measurements were performed with a Scintag, XDS 2000 powder diffractometer, with a copper 1.54 Å radiation source. A liquid nitrogen cooled germanium solid state detector was used to capture the scattered x-rays. The experimental, technical parameters of the instrument are listed in Table II.

RESULTS AND DISCUSSION

Crystallization of PET/MXD6 blends under dynamic cooling

In the case of a typical exothermic crystallization curve obtained with a DSC, the initial temperature at which the cooling curve first deviates from the baseline is sometimes taken as a measurement of the onset of crystallization. An additional temperature, referred to as the extrapolated initial temperature (T_{ie}), is obtained at the intercept of tangents to the baseline and the high temperature side of the exothermic peak. The crystallization peak temperature (T_p) is the temperature at which maximum crystallization occurs. The quantity (T_{ie}–T_p) is; therefore, a

TABLE II
Technical Parameters Utilized for the X-Ray Measurements

KV	40
MA	35
Slit distance	2, 4, 0.5, 0.3
Start angle	10°
End angle	60°
Step size	0.02°
Scan rate	2.5
Scan mode	Continuous
Wavelength	1.541838 nm
Tube	Type: fixed slits
Detector	Type: fixed slits
	Offset: 0.000000

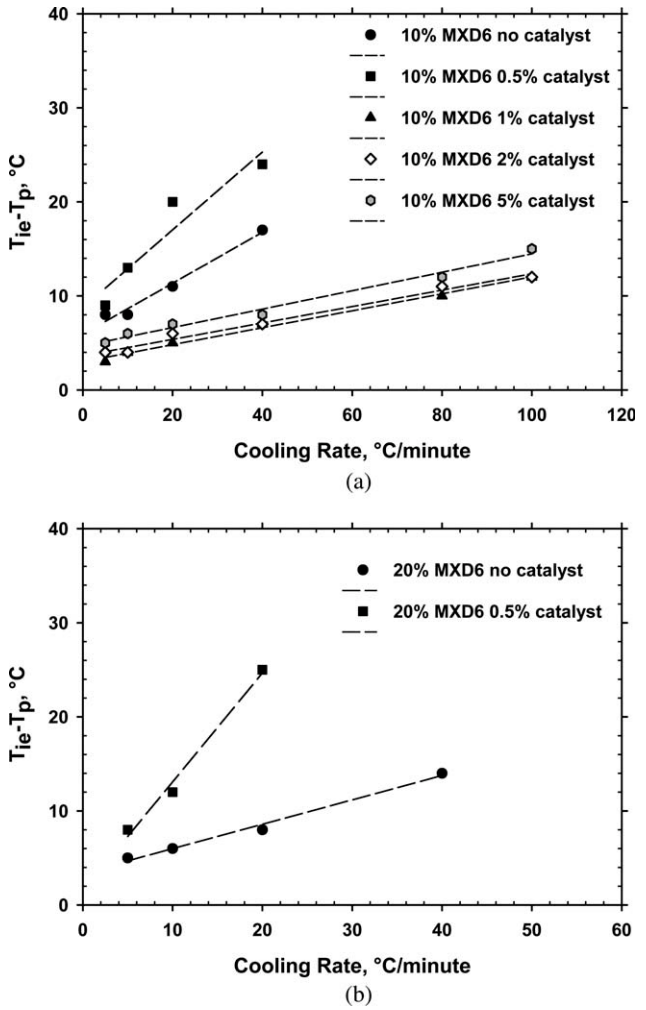

Figure 1 Overall rates of crystallization are illustrated in terms of (T_{ie}–T_p) values plotted as functions of cooling rates, for PET/MXD6 blends prepared with (a) 10% MXD6 with 0–5% catalyst (b) 20% MXD6 with 0–0.5% catalyst.

function of the overall rate of crystallization, the smaller the difference between these temperatures, the faster the rate of crystallization.[53]

PET/MXD6 blends, containing 10 or 20% MXD6 and various catalyst concentrations, were cooled in a DSC at rates from 5 to 100°C per minute to examine their dynamic crystallization behaviors. Figure 1(a,b) illustrates the relationships between (T_{ie}–T_p) and cooling rates for these blends. It can be seen that as cooling rates are increased higher (T_{ie}–T_p) values are obtained for all samples, indicating broader crystallization exotherms. These figures also illustrate the effects of sodium *p*-toluene sulfonate catalyst on the PET/MXD6 blends. Figure 1(a) gives values for 10% MXD6 blends with catalyst concentrations from 0 to 5%. It can be seen that the highest (T_{ie}–T_p) values are exhibited by blends containing 0.5% catalyst. This behavior indicates that samples with a 0.5% catalyst concentration crystallize more slowly than blends without catalyst, as well as the blends containing higher catalyst concentrations. Figure 1(b) shows similar results for 20% MXD6 blends containing 0 and 0.5% catalyst. The 10% MXD6 blends that contain higher levels of catalyst exhibit much lower (T_{ie}–T_p) values than those with either 0 or 0.5%, indicating relatively faster rates of crystallization.

Figure 2 gives peak crystallization temperatures measured for 10% MXD6 blends containing up to 5% catalyst and 20% MXD6 blends containing 0 and 0.5% catalyst. In this case, higher peak crystallization temperatures indicate a greater tendency to crystallize, while being cooled from the melt. As with the (T_{ie}–T_p) results, samples containing 1, 2 and 5% catalyst are seen to crystallize more readily than those containing 0 and 0.5% catalyst.

In the previous PET-MXD6 blend study,[52] it was concluded that higher catalyst contents resulted in higher levels of copolymer formation and higher degree of randomness values for the resulting PET-MXD6 copolymers. These results suggested that to improve the interfacial compatibility of PET/MXD6 blends; more catalyst should be added to the blends. The current crystallization results show that when the content of catalyst is higher than 0.5%, the catalyst not only catalyzes the ester-amide interchange reaction between PET and MXD6, but also acts as nucleating agent for the blends. This means when PET/MXD6 blends with higher catalyst contents are extruded, the final products will crystallize faster. More rapidly crystallizing blends would make it more difficult to prepare injection molded amorphous parts such as preforms for use in clear container blow molding applications.

The crystallization rates of blends with 0.5% catalyst are slower than those of blends without catalyst in terms of their (T_{ie}–T_p) values; however, their respective peak crystallization temperatures are more similar. This occurs because the blend samples

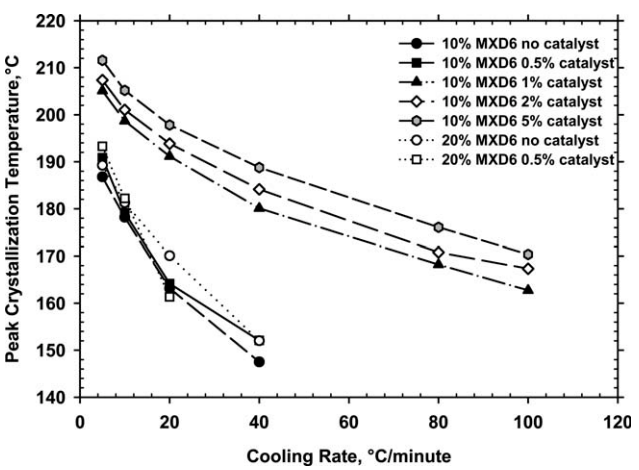

Figure 2 Crystallization peak temperatures of PET/MXD6 blends containing 10 and 20% MXD6, prepared without catalyst and with catalyst concentrations up to 5%.

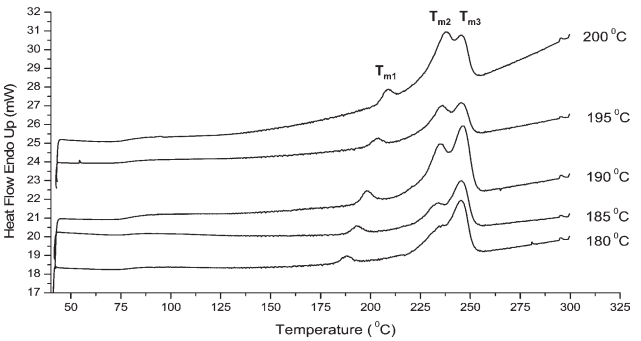

Figure 3 An example of changes in the positions of multiple melting peaks (T_{m1}, T_{m2}, and T_{m3}) observed for an uncatalyzed blend containing 10% MXD6 and 90% PET and isothermally crystallized at the indicated temperatures.

containing 0.5% catalyst begin to crystallize at slightly higher temperatures than those without catalyst. They then continue to crystallize, but more slowly than those containing 1–5% catalyst and exhibit peak crystallization temperatures similar to those of the uncatalyzed blends. The reason for this is the presence of the PET-MXD6 copolymer. PET chains with the attachments of MXD6 segments move with more difficultly than the PET chain without the hindrance of MXD6 segments. As a result, the overall crystallization rate is slowed.

The catalyst has two effects on PET/MXD6 blends. One is a catalyzing effect; the other is a nucleation effect. Both of them depend on the content of catalyst in the blends. When the content of catalyst is 0.5% or lower, the nucleating effect of the catalyst on the blends is not as prominent. Its major effect is the catalyzing effect to produce higher concentrations of copolymer through the ester-amide interchange reaction between PET and MXD6. When the content of catalyst is higher than 0.5%, the major effect is nucleation.

Equilibrium melting point and crystallization behavior of PET/MXD6 blends

The equilibrium melting temperature (T_m^0) of a crystallizable polymer is important for determination of degree of supercooling; since it is used as a reference temperature from which the driving force for crystallization is observed. Equilibrium melting temperatures were; therefore, determined for each of the PET/MXD6 blends, as well as for the unblended polymers.

PET that has been isothermally crystallized at temperatures from 180 to 205°C will generally exhibit three melting peaks, when it is reheated at a programmed rate. These peaks have been designated as T_{m1}, T_{m2}, and T_{m3}. Isothermally crystallized MXD6 has been found to exhibit two melting peaks, when crystallized in the lower temperature range from 170 to 180°C. In the higher crystallization temperature range, from 185 to 195°C, it displays three melting peaks. While there are many different interpretations of the observed multiple melting peaks, a common interpretation is that the first melting peak T_{m1} is associated with the temperature used for isothermal crystallization and may represent small portions of metastable crystalline material. The third peak (T_{m3}) has been said to represent the reorganization and recrystallization that occurs during heating at a programmed rate in a DSC. The second melting peak (T_{m2}) has been taken to represent the quality of crystalline structures formed during primary crystallization. This peak is used to provide data used for extrapolation to the intercept (T_m^0) with a theoretical line constructed from equivalent melting and crystallization temperatures.

Figure 3 shows examples of T_{m1}, T_{m2}, and T_{m3} observed in the melting curves of isothermally crystallized 90% PET/10% MXD6 blends prepared without catalyst. Similar additional DSC curves were obtained for these and the other crystallized blend samples. The occurrences of these three melting peaks are related to the melting of crystalline components in the PET/MXD6 blends. The temperatures of peaks T_{m1}, T_{m2}, and T_{m3} (of the 90% PET/10% MXD6 blends prepared without catalyst) have been plotted as functions of crystallization temperature in Figure 4. It can be seen that with increasing isothermal crystallization temperatures, the positions of T_{m1} and T_{m2} shift to higher temperatures. The position of T_{m3} is relatively constant. This is consistent with results obtained by Zhou and Clough.[6] From Figure 4, if we extrapolate the T_{m2} line to higher temperatures, it will intercept with the $T_m = T_c$ line. On the

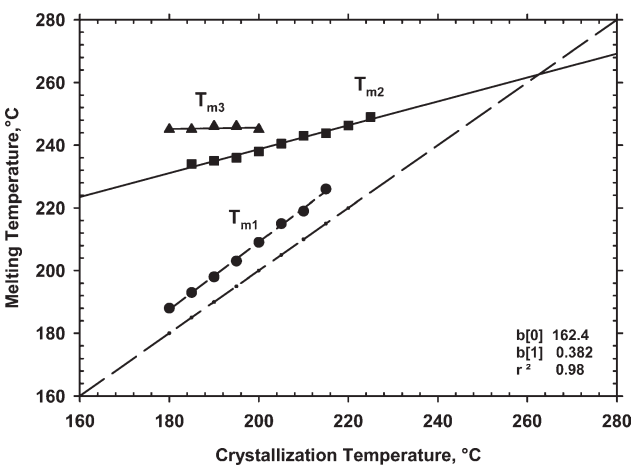

Figure 4 Changes in T_{m1}, T_{m2}, and T_{m3} are plotted as functions of isothermal crystallization temperatures for an uncatalyzed blend containing 10% MXD6 and 90% PET. Extrapolation of the T_{m2} line is used for determination of T_m^0.

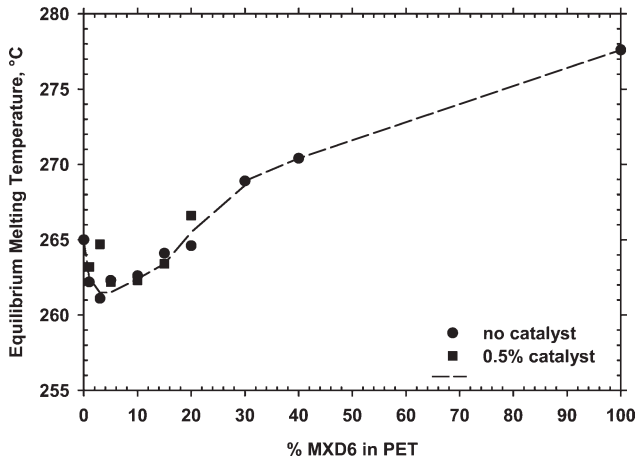

Figure 5 Changes in the equilibrium melting temperatures of PET/MXD6 blends with 0 and 0.5% catalyst are plotted as functions of their MXD6 contents.

basis of the calculation method of Hoffman and Weeks,[54] the intercept is the equilibrium melting point (T_m^0), as they have shown in eq. (1).

$$T_m = T_m^0(1 - 1/\gamma) + T_c/\gamma \quad (1)$$

Similar experimental procedures and calculations were carried out for the PET, MXD6, and various blends. Figure 5 gives an overview of the equilibrium melting temperatures calculated for PET/MXD6 blends prepared with both 0 and 0.5% catalyst. It can be seen that if the content of MXD6 is in the range from 3–5% in the PET/MXD6 blends, the equilibrium melting point (T_m^0) is lower than that of unblended PET. If MXD6 concentrations are above 5%, T_m^0 increases with increased levels of MXD6. Similar changes are observed for samples both with and without catalyst.

Depression of the equilibrium melting point of a crystalline polymer can result from different factors. As suggested by Nishi and Wang,[36] for crystalline/amorphous systems, the equilibrium melting point of the crystalline phase will be depressed with an increased content of the amorphous component in the blends. This phenomenon is similar to the melting point depression observed in crystalline polymer/diluent systems. Generally, the depression in the equilibrium melting point of a crystalline polymer blended with an amorphous polymer provides important information about its miscibility and its associated polymer–polymer interaction parameter.

For the case of an immiscible or partially miscible blend, depression of the equilibrium melting point is not generally observed. In the case of a miscible blend; however, the equilibrium melting point can be depressed with increasing content of the amorphous polymer in the blend. This is especially true for miscible blends in which specific interactions occur between the components. The equilibrium melting point of a polymer is affected not only by thermodynamic factors, but also by morphological factors such as crystalline lamellar thickness.

Values for the morphological factor can be obtained from the previously described equilibrium melting point data. According to eq. (1) from Hoffman and Weeks,[54] the morphological factor (γ) is the reciprocal of the slope of the extrapolated T_{m2} line, as illustrated in Figure 4. This factor indicates changes in chain-folded lamellar thickness, resulting from crystallization; with γ representing the ratio of initial to final lamellar thickness. Table III gives γ values for the blends and unblended polymers, prepared with and without catalyst. The measured equilibrium melting temperatures are also included. Changes of the γ values are very small; however, it can be seen that they increase slightly at low concentrations of MXD6 and then continuously decrease as MXD6 concentrations exceed 10%.

The Flory-Huggins interaction parameter(χ_{12}) plays an important role on the melting behavior of the crystalline and amorphous polymer system, since depression of the equilibrium melting point can be realized only if χ_{12} is negative. A plot was prepared following the Flory-Hugging theory for the thermodynamic mixing and using the equation developed by Nishi and Wang[36] with modifications by Scott.[55] These results are not presented; however, since the reductions in T_m^0 are very small and within such a narrow range (from 3–5% MXD6) that they do not yield a reasonable interpretation of the data.

The observed changes in equilibrium melting temperatures, observed in Figure 5, may be explained in terms of eutectic phase changes. This behavior has been well described by other researchers.[56–59] In particular, Cason and Rapoport[56] discuss these phase changes in terms of solid and liquid phases and relative rates of each individual component to change phase in the presence of the other. According to their discussions, at a material's melting temperature

TABLE III
Morphological Factors (γ) Calculated for Blends Prepared Without Catalyst and Containing 0.5% Catalyst

% MXD6	No catalyst T_m^0	γ	0.5% catalyst T_m^0	γ
0	265.0	2.57	–	–
1	262.2	2.67	263.2	2.61
3	261.1	2.75	264.7	2.54
5	262.3	2.60	262.2	2.65
10	262.6	2.62	262.3	2.69
15	264.1	2.46	263.4	2.63
20	264.6	2.41	266.6	2.62
30	268.9	2.17	–	–
40	270.4	2.08	–	–
100	277.6	1.61	–	–

molecules from the solid and liquid phase exist in equilibrium with each other. They describe this in terms of the escaping tendency of molecules from the solid phase being equal to the escaping tendency of molecules from the liquid phase. In terms of the current work; as the PET concentrations are reduced from 100 to 95% (wt/wt), molecules in the solid (crystalline) PET phase continue to escape to the liquid (amorphous) phase as though they were still at concentrations of 100%. In the liquid phase; however, the presence of liquid (amorphous) MXD6 reduces the rate of escape of the liquid PET molecules to return to the solid phase. As this occurs, the equilibrium melting transition between solid and liquid is reduced. This is illustrated by the reductions in equilibrium melting temperatures toward the left side of Figure 5.

As concentrations of MXD6 exceed 5% (PET concentrations less than 95%) it can be seen that T_m^0 increases. This also can be explained in terms eutectic phase changes. With increasing concentrations of MXD6, portions of the MXD6 begin to crystallize as does the PET. This crystallization reduces the concentrations of MXD6 in the liquid (amorphous) phase, thus permitting the PET molecules to escape more readily from the liquid phase, raising T_m^0. At concentrations exceeding the eutectic point both polymer materials crystallize. It is expected that a second eutectic point might be present at very high concentrations of MXD6 and very low concentrations of PET. Experiments to determine if this would occur; however are outside the scope of this research.

Similar descriptions of eutectic phase changes have been well documented by numerous researchers. Hirami and Matsuda[57] derived a general melting temperature equation for binary mixture systems with two crystallizable components and demonstrated its application with binary mixture data for polyethylene and normal alkane as well as for nylon 6 and nylon 66. They also included schematic diagrams to illustrate phase changes of the various components in the binary mixtures. Matkar and Kyu[58,59] have extensively studied the various phase interactions of polymer blends and have developed a self-consistent theory for determination of phase diagrams that consider the possible amorphous-amorphous, crystal-amorphous, amorphous-crystal, and crystal–crystal interactions. Their predicted phase diagrams have been compared with reported blend data including that for polyvinylidene fluoride (PVDF) and PMMA, PCL and low molecular weight polystyrene, polyethylene fractions, as well as PCL and trioxane mixtures.

Applications of the above concepts to current blends of MXD6 with PET indicate that in Figure 5, areas above the lines connecting the data points are composed of liquid (amorphous) PET and liquid (amorphous) MXD6. Areas below the descending line, at MXD6 concentrations below 3–5%, and temperatures from 261 to 265°C are composed of liquid (amorphous) PET, solid (crystalline) PET, and liquid (amorphous) MXD6. No solid (crystalline) MXD6 would be present in this region. As concentrations of MXD6 increase, the area under the curve following these changes from temperatures of 262 to 278°C should include solid (crystalline) MXD6 as well as the other three components. At very high concentrations of MXD6 a second eutectic point might occur. In this case the components to the right of this point should include liquid (amorphous) MXD6, solid (crystalline) MXD6, and liquid (amorphous) PET.

Samples prepared for equilibrium melting temperature measurements were crystallized isothermally after being cooled from the melt to temperatures from 180 to 225°C. The crystallization half time values obtained for these samples (containing 0 and 0.5% catalyst) are plotted as functions of degree of supercooling in Figure 6(a,b). Degree of supercooling or undercooling is the difference between the equilibrium melting point of the polymer and the crystallization temperature ($T_m^0 - T_c$) and is a major factor controlling the crystallization of polymers. The crystallization half time ($t_{1/2}$) is the time at which a polymer achieves a value equal to 50% of its final level of crystallinity. The crystallization half time can reflect the overall crystallization rate of the polymer, with a smaller half time indicating a faster crystallization rate. As can be seen in Figure 6(a,b), all samples show smaller crystallization half times with increased degrees of undercooling. It is also evident that at the same degree of undercooling, blends with various MXD6 contents exhibit crystallization half times that are similar to each other and lower than those of equivalent unblended PET. This is because the dilution effect of the amorphous component leads to the increase of the crystallization rate of the PET/MXD6 blends.

X-ray diffraction of PET/MXD6 blends

Thermal results obtained for PET/MXD6 blends have clearly shown that crystallization occurs as a result of dynamic cooling and isothermal exposures at elevated temperatures. It is therefore important to determine which of the blend components forms the crystalline phase in the variously prepared PET/MXD6 blend systems. X-ray diffraction has been used by others to determine that the crystalline forms of both MXD6 and PET are triclinic with unit cell dimensions of $a = 1.201$ nm, $b = 0.483$ nm, and $c = 2.98$ nm in the case of MXD6.[60] The unit cell dimensions of PET are $a = 0.450$ nm, $b = 0.590$ nm, and $c = 1.076$ nm.[61,62] For this work; however, a

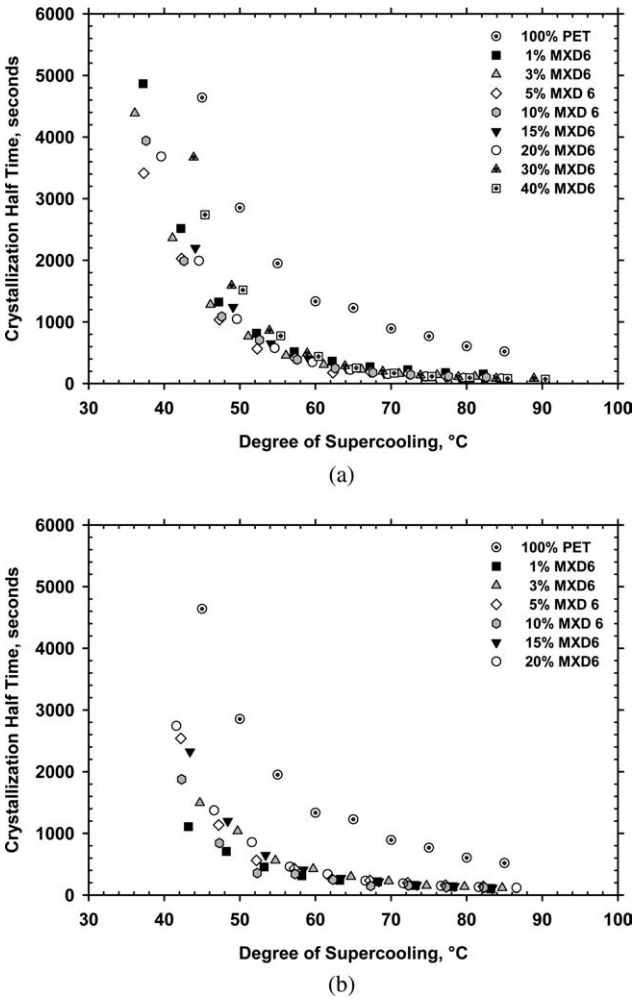

Figure 6 Crystallization half times are plotted as functions of degree of supercooling for blend samples containing various concentrations of MXD6 and prepared (a) without catalyst and (b) with 0.5% catalyst.

wide-angle x-ray diffraction technique has been used to measure the diffraction peaks of each crystalline component, as a direct method to detect the natures of the crystalline phases in the blends. Table IV lists the diffraction angles and peak positions that have been assigned to the unblended PET and MXD6 polymers.

TABLE IV
Crystal Plane Positions in Unblended PET and MXD6

PET		MXD6	
2θ (°)	Index of crystal plane	2θ (°)	Index of crystal plane
16.48	$0\bar{1}1$	–	–
17.50	010	18.84	100
21.79	$\bar{1}11$	21.49	110
22.82	$1\bar{1}0$	–	–
26.04	100	25.56	010
32.78	$1\bar{1}1$	–	–

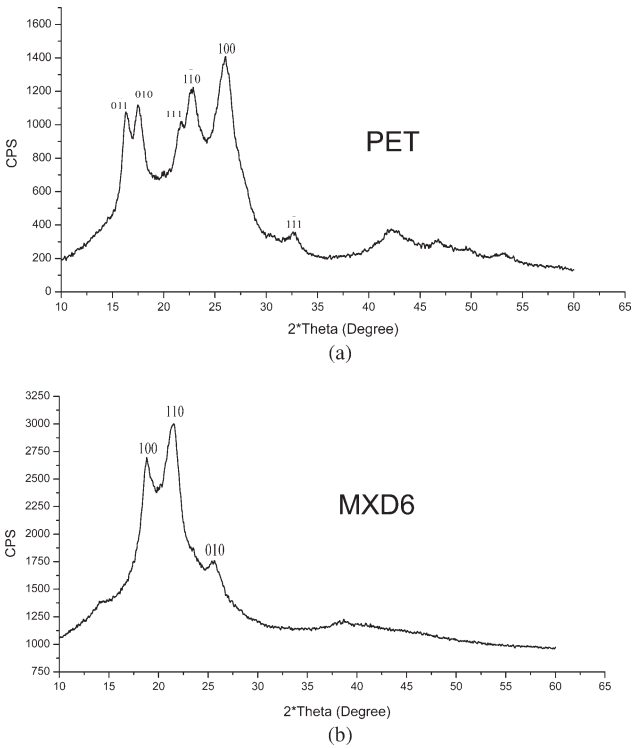

Figure 7 X-ray diffraction scans of (a) PET and (b) MXD6 illustrating the positions of their main diffraction peaks.

Figure 7(a) displays a typical x-ray diffraction scan of crystallized PET. Six different crystal planes have been indexed on the basis of the reciprocal lattice of a PET crystal in the scan. A typical scan of crystallized MXD6 is given in Figure 7(b), indicating the positions of its three main diffraction peaks. By monitoring the positions and occurrences of the diffraction peaks of each crystalline blend, one can determine whether the PET or MXD6 component is present in the crystalline phase. Figure 8(a) shows that when the content of MXD6 is lower than 10% in the blends prepared without catalyst, the diffraction scans are similar to that of PET. At these lower concentrations, the presence of MXD6 in the blends does not change the shapes of the diffraction scans. All of the scans have the same diffraction peaks as recorded for pure PET. The positions of the diffraction peaks in blends containing 1–5% MXD6 do not change. In the case of the blend containing 10% MXD6, the diffraction peaks shift to a very slightly higher angle (about 1 degree). These results indicate that the PET crystallizes, while the MXD6 does not. Uncatalyzed blends of PET/MXD6 with MXD6 contents lower than 10%, prepared under equivalent crystallization conditions, primarily exhibit crystalline/amorphous type morphologies. In these blends, PET comprises the major portion of the crystalline phase and MXD6 remains in the amorphous phase.

In the case of an uncatalyzed 20% MXD6/80% PET blend (not shown), the x-ray diffraction scan is

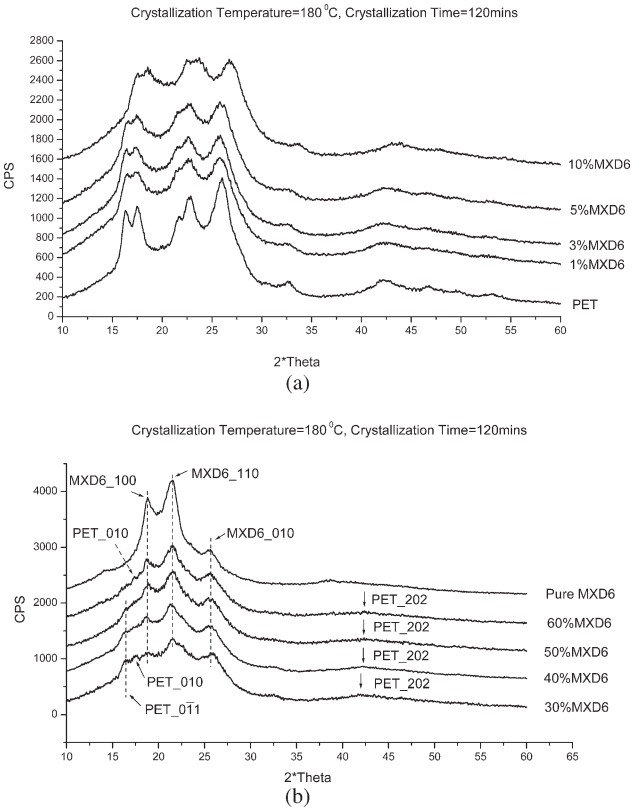

Figure 8 X-ray diffraction scans are shown for PET/MXD6 blends, crystallized at 180°C for 2 h. (a) The scans of blends containing 0–10% MXD6 indicate little change from that of pure PET. (b) The scans representing blends containing 30–100% MXD6 indicate crystallization of the MXD6 as well as the PET, if present.

also similar to that of PET; however, the presence of the higher MXD6 content leads to the widening of the $\bar{1}11$ crystal plane peak. As was seen in Figure 8(a) for the blend with 10% MXD6, the peak width of $\bar{1}11$ crystal plane of the blends is almost the same as that of pure PET. This widening phenomenon is due to the crystallization of MXD6 component in the blends. Because the MXD6 crystallizes in the 20% MXD6 physical blend, the 110 crystal plane of MXD6 increases the size of the $\bar{1}11$ crystal plane from that seen for pure PET.

When the content of MXD6 is further increased, the morphologies of the blends continue to change. As shown in Figure 8(b), scans of blends with higher contents of MXD6 exhibit typical MXD6 diffraction peaks and also small PET diffraction peaks. In the case of the 30% MXD6 blend, the scan shows crystal planes $0\bar{1}1$ and 010 of PET. Spectra of 40 and 50% MXD6 blends show crystal plane $0\bar{1}1$ of PET and those of 40 and 60% MXD6 blends have the crystal plane 010 of PET. All of the blends exhibit crystal plane 202 of PET. The other diffraction peaks of the PET component cannot be clearly seen, because of overlapping peaks. These results indicate that when the content of MXD6 in the physical blends is higher than 10%, both the PET and MXD6 crystallize and display morphologies of the crystalline/crystalline type. In addition, it is expected that if the MXD6 content is higher than 90–95%, then the PET/MXD6 blend morphologies will change to an amorphous/crystalline system, in which the PET remains in the amorphous phase and the MXD6 provides the crystalline phase.

The previously discussed x-ray diffraction scans were obtained for various compositions of samples, crystallized for two hours at 180°C. Factors, in addition to composition, that could influence the morphologies of PET/MXD6 physical blends include crystallization temperature and crystallization times. To evaluate the effects of these variables, uncatalyzed blends containing 10 and 40% MXD6 were crystallized at 180°C for 10, 30, 60, 90, and 120 min. Similar additional samples were crystallized for 120 min at temperatures of 180, 190, 200, and 210°C. Examinations of the scans obtained for these blend compositions indicate that the shapes and positions of their specific diffraction peaks do not change as a result of exposure to these different crystallization times and temperatures. Figure 9 gives an example of diffraction scans obtained for samples containing 40% MXD6, held for 120 min at temperatures from 180 to 210°C.

In the case of lower contents of MXD6 (lower than 10%), the morphologies of the blends prepared without catalyst are primarily crystalline/amorphous, with PET as the crystalline phase and MXD6 in the amorphous phase. At higher MXD6 concentrations both phases are found to crystallize indicating crystalline/crystalline morphologies. If MXD6 concentrations constitute 90–95% or more of the blend composition morphologies are expected to be amorphous/crystalline with PET in the amorphous phase. In addition, results indicate that the experimental crystallization temperatures and times do not change the shapes of the scans or the positions of the diffraction

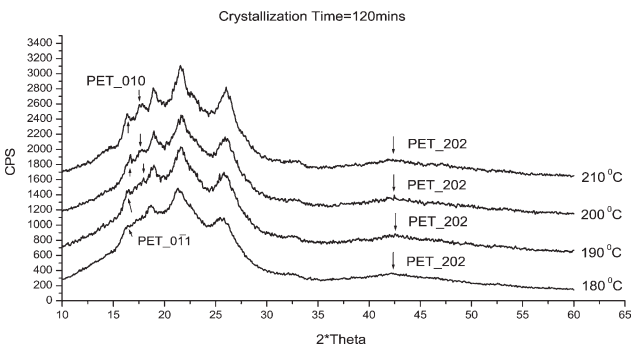

Figure 9 X-ray diffraction scans of PET/MXD6 blends, containing 40% MXD6 crystallized for 2 h at temperatures from 180 to 210°C. These scans indicate little change as a result of increased crystallization temperature.

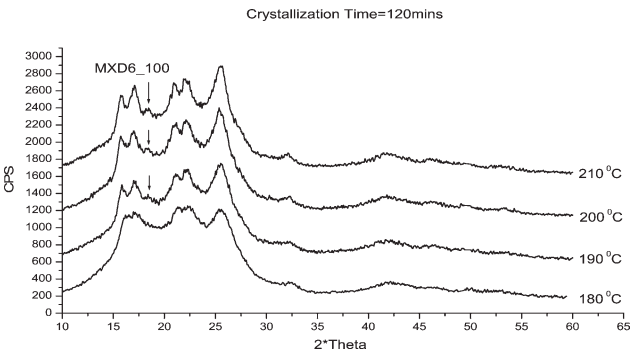

Figure 10 X-ray diffraction scans of PET/MXD6 blends, containing 0.5% catalyst, crystallized for 2 h at temperatures from 180 to 210°C. These scans indicate that the MXD6 is crystallizing at temperatures above 180°C.

peaks. Under the specified crystallization conditions, the morphologies of each blend remains constant, indicating that each component is crystallizing independently of the other. There is no evidence that co-crystallization of the PET and MXD6 has occurred.

The addition of catalyst to the blends was previously found to induce an interchange reaction between PET and MXD6 in the blends.[52] The possible influence of the interchange reaction on the morphologies of the blends should; therefore, also be considered. Figure 10 displays diffraction scans, of 10% MXD6/90% PET blends prepared with 0.5% catalyst and crystallized at temperatures from 180 to 210°C. As with the uncatalyzed blends, samples crystallized at 180°C exhibit diffraction peaks indicating crystallization of primarily the PET blend component. When the crystallization temperature is higher than 180°C; however, the crystal plane 100 of MXD6 appears in the scans; indicating that at the higher temperatures the MXD6 as well as the PET has crystallized. The morphologies of blends containing 0.5% catalyst and crystallized at temperatures above 180°C; therefore, appear to be of the crystalline/crystalline rather than the crystalline/amorphous type. Similar experiments, performed using 10% MXD6/90% PET blends prepared without catalyst, did not exhibit a clear peak to indicate crystallization of the MXD6 component after 120 min at temperatures from 180 to 210°C. These results indicate that the catalyst has a nucleating effect on the blend and has produced in an increased tendency of the MXD6 to crystallize at temperatures from 190 to 210°C. It should also be noted that levels of PET MXD6 copolymer present in catalyzed blends are very small, as discussed in the previous article.[52] This copolymer would; therefore, be expected to remain in the amorphous phases of the blends rather than contribute to any observed crystallinity. This expectation is supported by the fact that no peaks, in addition to those assigned to PET and MXD6, have been observed in the x-ray diffraction scans of the blends.

The above x-ray diffraction results are consistent with the thermal analysis results previously discussed in terms of blend (T_{ie}–T_p) values. The DSC data had shown that crystallization rates of samples containing 0.5% catalyst are slower than those without catalyst. The differences in (T_{ie}–T_p) values occur because the blend samples containing 0.5% catalyst begin to crystallize (T_{ie}) at slightly higher temperatures than those without catalyst and continue to crystallize more slowly, reaching peak (T_p) crystallization values similar to those of uncatalyzed blends. This broad crystallization is indicated by the higher (T_{ie}–T_p) values, which occur in part as a result of the nucleating effects of the catalyst which cause higher (T_{ie}) values. Samples containing higher catalyst concentrations exhibited both higher temperature (T_{ie}) and (T_p) values, yielding smaller differences in (T_{ie}–T_p), because of their sharper peaks and much faster rates of crystallization. Any PET-MXD6 copolymer present as a result of the interchange reaction would have been expected to somewhat inhibit crystallization of the blend samples. The catalyst; however has created a competing effect by acting as a nucleating agent to facilitate crystallization of both blend components.

PET crystallite size in PET/MXD6 blends

In the previous sections, we have discussed the morphological changes of PET/MXD6 blends with and without catalyst. Discussions will now include the changes of the PET crystallite sizes as a result of blend composition. The crystallite size was calculated by using the Scherrer[63] equation as shown in eq. (2).

$$L_{hkl} = \frac{K\lambda}{\beta_0 \cos(\theta)} \tag{2}$$

where L_{hkl} is the crystallite size perpendicular to plane *hkl*, *h*, *k*, and *l* are the Miller indices. *K* is the constant commonly assigned a value of 1, λ is the wavelength of light, β_0 is the integral breadth or breadth at half-maximum intensity, and θ is the scattering angle. In eq. (2), the constant (*K*) was assigned a value of 1 for all samples. Since the unit cell of PET crystals is triclinic, the reciprocal lattice vector is not necessarily aligned along the crystallite chain axis. The lattice vector; however, is proportional to the projection on the crystallite chain axis giving an effective or apparent crystallite size. As we know, the true driving force for crystallization is not the crystallization temperature, but rather the degree of undercooling. The degree of undercooling is taken as the equilibrium melting temperature minus the crystallization temperature. Figure 11(a,b) shows crystallite sizes plotted as functions of the degree of undercooling.

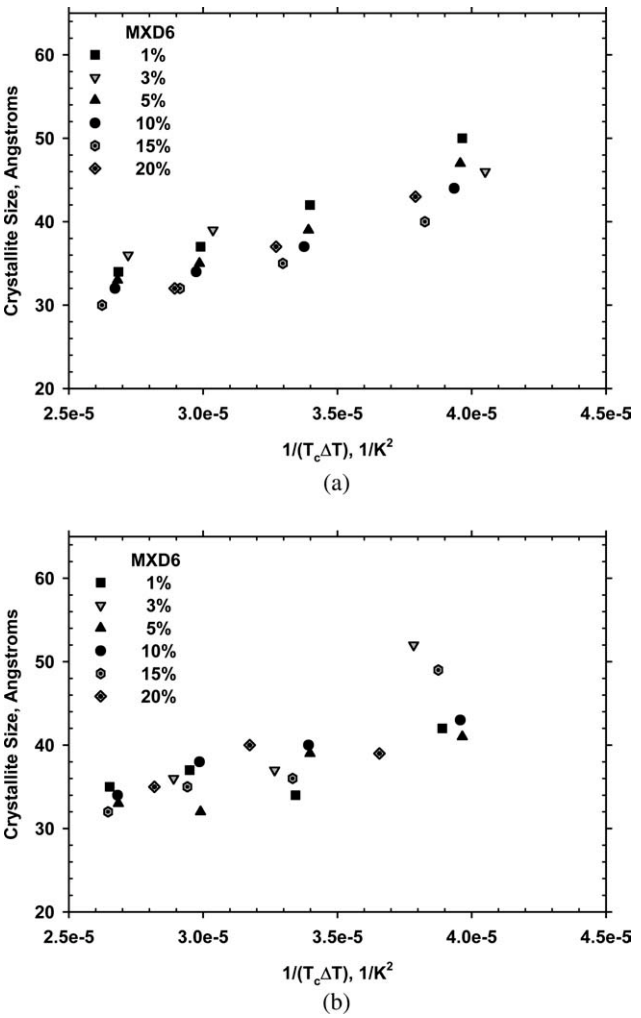

Figure 11 The relationship of the crystallite size of the 100 plane of PET/MXD6 blends to the degree of undercooling for samples containing various concentrations of MXD6 and prepared (a) without catalyst or (b) with 0.5% catalyst.

With the decrease of the degree of undercooling, the crystallite sizes of PET/MXD6 blends both with and without catalyst increase. For the PET/MXD6 blends without or with catalyst, as shown in Figure 11(a,b), the changes of MXD6 contents in the blends result in the changes of the crystallite sizes, but these changes are also very small. The contents of MXD6 in the blends have no significant influence on the values of the crystallite size of PET crystals in PET/MXD6 blends with and without catalyst. The main factor which can affect the crystallite sizes in the blends is the degree of undercooling.

CONCLUSIONS

Melting and crystallization behavior of PET/MXD6 blends prepared with and without catalyst have been discussed. The phase characteristics have been investigated for the PET/MXD6 blends under various isothermal crystallization conditions. The equilibrium melting point T_m^0 and morphological factor (γ), have been introduced to characterize the melting and crystallization behavior of PET/MXD6 blends. The relationships between the crystallite sizes and the degrees of undercooling have also been investigated. The conclusions are as follows:

1. The catalyst in the PET/MXD6 blends has both a catalyzing and nucleation effect. Higher content of catalyst leads to faster crystallization rates of the PET/MXD6 blends.
2. In the crystallization temperature range between 180 and 220°C, when the content of the MXD6 is lower than 3–5% in the PET/MXD6 blends with or without catalyst, PET crystallizes and MXD6 does not crystallize. Within the concentration range evaluated, when the MXD6 content is higher than 5%, PET and MXD6 both crystallize.
3. The main factor that affects the crystallite size of the blends is the degree of undercooling, rather than the blend composition.
4. X-ray diffraction results indicate that uncatalyzed PET/MXD6 blends are crystalline/amorphous systems when the MXD6 content is lower than 3–5%. These blends comprise crystalline/crystalline systems when the MXD6 contents are higher than 5–10%. At MXD6 concentrations above 90–95% the MXD6 is expected to be crystalline while the PET phase is amorphous.
5. The presence of only 0.5%, catalyst in the blends acts as a nucleating agent and causes the MXD6 as well as the PET to crystallize, when MXD6 concentrations are as low as 10% and exposure temperatures exceed 180°C.

References

1. Kong, Y.; Hay, J. N. Polymer 2004, 44, 624.
2. Gao, Q.; Tang, Z. L.; Huang, N. X.; Gerkin, L. J Appl Polym Sci 1998, 69, 729.
3. Roberts, R. C. Polym Lett 1970, 8, 481.
4. Nealy, D. L.; Davis, T. G.; Kibler, C. J. J Polym Sci: Part A-2 1970, 8, 2141.
5. Fakirov, S.; Fisher, E. W.; Hoffman, R.; Schmidt, G. F. Polymer 1977, 18, 1121.
6. Zhou, C.; Clough, S. B. Polym Eng Sci 1988, 28, 65.
7. Sweet, G. E.; Bell, J. P. J Polym Sci: Part A-2 1972, 10, 1274.
8. Holdsworth, P. J.; Turner-Jones, A. Polymer 1971, 12, 195.
9. Groeninckx, H.; Reynaers, H.; Berghmans, H.; Smets, G. J Polym Sci: Polym Phys Ed 1980, 18, 1411.
10. Groeninckx, H.; Reynaers, H. J Polym Sci: Polym Phys Ed 1980, 18, 1425.
11. Wunderlich, B. Macromolecular Physics; Academic Press: New York, 1980; Vol. 3.
12. Bassett, D. C.; Olley, R. H.; Al Raheil, I. A. M. Polymer 1988, 29, 1745.

13. Blundell, D. J. Polymer 1987, 28, 2248.
14. Lattimer, M. P.; Hobbs, J. K.; Hill, M. J.; Barham, P. J. Polymer 1992, 44, 4971.
15. Lee, Y. C.; Porter, R. S. Macromolecules 1987, 20, 1446.
16. Verma, R.; Marand, H.; Hsiao, B. Macromolecules 1996, 29, 7767.
17. Cheng, S. Z. D.; Wunderlich, B. Macromolecules 1986, 19, 1868.
18. Cheng, S. Z. D.; Wunderlich, B. Macromolecules 1988, 21, 789.
19. Talibuddin, S.; Wu, L.; Runt, J. Macromolecules 1996, 29, 7527.
20. Alfonso, G. C.; Russell, T. P. Macromolecules 1986, 19, 1143.
21. Benjamin, S. H.; Bryan, B. S. J Polym Sci: Part B: Polym Phys 1993, 31, 901.
22. Cheung, Y. W.; Stein, R. S. Macromolecules 1993, 26, 5365.
23. Cheung, Y. W.; Stein, R. S. Macromolecules 1994, 27, 2520.
24. Cheung, Y. W.; Stein, R. S. Macromolecules 1994, 27, 2512.
25. Cheung, Y. W.; Stein, R. S. Macromolecules 1994, 27, 3585.
26. Eguiazabal, J. I.; Iruin, J. J. Polym Bull 1990, 24, 641.
27. Huo, P. P.; Cebe, P. Macromolecules 1993, 26, 3127.
28. Fakirov, S.; Sarkissova, M.; Denchev, Z. Macromol Chem Phys 1996, 197, 2837.
29. Denchev, Z.; Sarkissova, M.; Fakirov, S.; Yilmaz, F. Macromol Chem Phys 1996, 197, 2869.
30. Fakirov, S.; Sarkissova, M.; Denchev, Z. Macromol Chem Phys 1996, 197, 2889.
31. Eguiazabal, J. I.; Cortazar, M.; Iruin, J. I. J Appl Polym Sci 1991, 42, 489.
32. Shi, Y.; Jabarin, S. A. J Appl Polym Sci 2001, 81, 23.
33. Shi, Y.; Jabarin, S. A. J Appl Polym Sci 2001, 81, 11.
34. Chen, H. L.; Li, L. J.; Lin, T. L. Macromolecules 1998, 31, 2255.
35. Morra, B. S.; Stein, R. S. J Polym Sci: Polym Phys Ed 1982, 20, 2261.
36. Nishi, T.; Wang, T. T. Macromolecules 1975, 8, 909.
37. Gorrasi, G.; Pucciariello, R.; Villani, V.; Vittoria, V.; Belviso, S. J Appl Polym Sci 2003, 90, 3338.
38. Liu, A. S.; Liau, W. B.; Chiu, W. Y. Macromolecules 1998, 31, 6593.
39. Tashiro, K.; Stein, R. S.; Hsu, S. L. Macromolecules 1992, 25, 1801.
40. Liau, W. B.; Liu, A. S.; Chiu, W. Y. Macromol Chem Phys 2002, 203, 294.
41. Qiu, Z. B.; Ikehara, T.; Nishi, T. Polymer 2004, 44, 2799.
42. Campoy, I.; Gomez, M. A.; Marco, C. Polymer 1999, 40, 4259.
43. Liu, Z. H.; Marechal, P.; Jerome, R. Polymer 1997, 48, 5149.
44. Chiu, H. J.; Chen, H. L.; Lin, J. S. Polymer 2001, 42, 5749.
45. Avella, M.; Martuscelli, E. Polymer 1988, 29, 1731.
46. Chen, H. L.; Wang, S. F. Polymer 2000, 41, 5157.
47. Escala, A.; Balizer, E.; Stein, R. S. Polym Prepr 1978, 19, 152.
48. Penning, J. P.; Manley, R. St J Macromolecules 1996, 29, 77.
49. Penning, J. P.; Manley, R. St J Macromolecules 1996, 29, 84.
50. Fujita, K.; Kyu, T.; Manley, R. St J Macromolecules 1996, 29, 91.
51. Guo, P.; Chang, C.; Morton, M. D. Polym Adv Technol 1995, 7, 168.
52. Xie, F.; Kim, Y. W.; Jabarin, S. A. J Appl Polym Sci 2009, 112, 3449.
53. Beck, H. N.; Ledbetter, H. D. Polym Chem Prepr 1964, 5, 824.
54. Hoffman, J. D.; Weeks, J. J. J Res Natl Bur Std 1962, 66, 13.
55. Scott, R. L. J Chem Phys 1949, 17, 279.
56. Cason, J.; Rapoport, H. Laboratory Text in Organic Chemistry, 2nd ed.; Prentice-Hall, Inc.: Englewood Cliffs, New Jersey, 1950; p 1962.
57. Hirami, M.; Matsda, T. Polym J 1999, 31, 801.
58. Matkar, R. A.; Kyu, T. J Phys Chem B 2006, 110, 12728.
59. Matkar, R. A.; Kyu, T. J Phys Chem B 2006, 110, 16059.
60. Ota, T.; Yamashita, M.; Yoshizaki, O.; Nagai, E. J Polym Sci (A-2) 1966, 4, 959.
61. Daubeny, R. P.; Bunn, C. W.; Brown, C. J Proc R Soc 1954, 226, 531.
62. Fakirov, S.; Fisher, E. W.; Schmidt, G. F. Makromol Chem 1975, 176, 2459.
63. Alexander, L. E. X-ray Diffraction Methods in Polymer Science; Wiley-Interscience: New York, 1969.